Norwegian Meteorological Institute

METreport

No. 07/2021
ISSN 2387-4201
Free

seNorge observational gridded datasets

seNorge_2018, versions 21.09 and 21.10

Cristian Lussana

The Norwegian Meteorological Institute, Oslo, Norway

Norwegian Meteorological Institute

METreport

Title	Date
seNorge observational gridded dataset. seNorge_2018, versions 21.09 and 21.10	October 9, 2021
Section	**Report no.**
Division for Climate Services	07/2021
Author(s)	**Classification**
Cristian Lussana	● Free ○ Restricted

Abstract

seNorge_2018 is an observational gridded dataset for daily aggregated temperatures and precipitation data over the Norwegian mainland. The time interval covered spans 65 years, from the 1st of January 1957 to the present day. Versions 21.09 and 21.10 (*v21*) of the historical archive 1957-2020 are described in this document, with special emphasis on the differences with respect to version 20.05 (*v20*).

Keywords

observational gridded datasets, temperature, precipitation, climatology, hydrology, statistical interpolation

Disciplinary signature
Hans Olav Hygen

Responsible signature
Cecilie Stenersen

Norwegian Meteorological Institute
Org.no 971274042
post@met.no
www.met.no / www.yr.no

Oslo
P.O. Box 43, Blindern
0313 Oslo, Norway
T. +47 22 96 30 00

Bergen
Allégaten 70
5007 Bergen, Norway
T. +47 55 23 66 00

Tromsø
P.O. Box 6314, Langnes
9293 Tromsø, Norway
T. +47 77 62 13 00

Contents

1 Introduction

seNorge indicates a collection of observational gridded datasets over Norway for daily mean, maximum and minimum temperature, and daily total precipitation amounts. The datasets are based on data from traditional weather stations and their predictions are available over a regular grid with 1 km spacing. The coordinate reference system is Universal Transverse Mercator, zone 33. The data sources used are: The Norwegian Meteorological Institute (MET Norway) climatological archive (frost.met.no), which includes also observations from stations managed by several public Norwegian institutions, such as The Norwegian Water Resources and Energy Directorate (NVE), the Norwegian Public Roads Administration (Statens vegvesen, SVV) and the Norwegian Institute of Bioeconomy Research (NIBIO); the Swedish Meteorological and Hydrological Institute (SMHI) climatological archive; Finnish Meteorological Institute (FMI) climatological archive. In addition, the daily datasets provided by the European Climate Assessment & Dataset project (ECA&D, https://www.ecad.eu, *Klein Tank et al.*, 2002) are used.

The in-situ data used has been quality controlled according to MET Norway's quality assurance system specifications. In addition, for temperature, a spatial consistency test has been applied *Lussana et al.* (2010); *Båserud et al.* (2020).

MET Norway started to produce the seNorge datasets versions 1.0 and 1.1 for the Norwegian mainland in the nineties (*Tveito and Førland*, 1999; *Tveito et al.*, 2000, 2002, 2005; *Mohr*, 2008). Version 2.0 has been available after 2015 (*Lussana et al.*, 2018b,a). The most recent seNorge member is seNorge_2018 (*Lussana et al.*, 2019), released in 2018 (version 18.12). This document describes versions 21.09 (September 2021) and 21.10 (October 2021). After the release of version 21.09, we discovered a problem with the aggregation of some of the observations used over Finland for the daily minimum and maximum temperatures, therefore we have adjusted these variables and released version 21.10 (only for daily minimum and maximum temperatures). Both versions 21.09 and 21.10 are abbreviated here as v21, that is: version 21.09 for precipitation and mean temperatures; version 21.10 for minimum and maximum temperatures.

The time period covered by the datasets begins the 1st of January 1957 (1957-01-01) and continues to the present day, with daily updates. seNorge_2018 datasets can be divided into two archives: an historical archive and an operational archive. The historical archive includes data from 1957-01-01 to a date in the recent past, which is 2020-12-31 for v21. The historical archive is re-built periodically. When a new version of the archive is created, each dataset gets its own Digital Object Identifiers (DOI). The operational archive is updated every day based on the data of the last few days. Each time a new historical archive is built, the operational archive is also modified, such that there is a seamless transition between the most recent version of the historical archive and the operational archive. In this sense, the operational archive is a provisional archive. For v21, the operational archive begins at 2021-01-01.

The spatial interpolation methods and the auxiliary information (e.g. topography, regional climate model monthly precipitation reference fields) used for v21 are the same as those used for v20, which have been described in the report by *Lussana* (2020).

The document is organized as follows. Sec. 2 defines v21 variables and presents the in-situ data used for spatial analysis. Sec. 3 compares v21 and v20 with the aim of studying the effects of variations of the input data over the results. Furthermore, we have conducted a comparison between the variables of v21 which refer to similar quantities, in order to quantify their differences. Sec. 4 summarizes the main messages of the document. The data access is then described in the Appendix. After the Appendix, a section with supplementary material is included, in order to make the reading of the main text more fluent by avoiding the interruptions caused by pages and pages of figures.

2 Data and Definitions

The definitions seNorge_2018 variables are:

- RR (daily precipitation) at a given date is the total amount of precipitation accumulated from 06 UTC of the day before that date to 06 UTC of the day in the date.
  - Pre-processing of in-situ data: observations are adjusted for the wind-induced under-catch according to the relationships reported by *Lussana et al.* (2019) and based on *Wolff et al.* (2015)
  - Post-processing of gridded fields: none
- TG (daily mean temperature) at a given date is the mean averaged temperature from 06 UTC of the day before that date to 06 UTC of the day in the date.
  - Pre-processing of in-situ data: outside Norway, the original daily mean temperature observations are used, without any modification. For Norwegian data, the observations used are the arithmetic mean of 24 hourly values, when they

are available, or a formula based mean value computed from fewer observations (*Førland and Tveito*, 1997). The equation used to obtain TG for a hypothetical *today* is:

$$
\begin{aligned}
TG &= 1/8 \cdot [T(\text{yesterday@06UTC}) + T(\text{today@06UTC}) + \\
&\quad +2 \cdot T(\text{yesterday@18UTC}) + \\
&\quad +2 \cdot Tmin(\text{from\_yesterday@18UTC\_to\_today@06UTC}) + \\
&\quad +2 \cdot Tmax(\text{from\_yesterday@18UTC\_to\_today@06UTC})]
\end{aligned}
$$

  - Post-processing of gridded fields: none

- TX (daily maximum temperature) at a given date is the maximum temperature from 18 UTC of the day previous to that date to 18 UTC of the day in the date.
  - Pre-processing of in-situ data: none
  - Post-processing of gridded fields: TX is consistent with TG and TN, such that TN $\leq$ TG $\leq$ TX

- TN (daily minimum temperature) at a given date is the minimum temperature from 18 UTC of the day previous to that date to 18 UTC of the day in the date.
  - Pre-processing of in-situ data: none
  - Post-processing of gridded fields: TN is consistent with TG and TX, such that TN $\leq$ TG $\leq$ TX

The new variables included in the v21 archive are:

- RRa is defined as RR but it is obtained without considering the adjustment for the wind-induced under-catch.
  - Pre-processing of in-situ data: none
  - Post-processing of gridded fields: none

- TM at a given date is the mean averaged temperature from 00 UTC to 24 UTC of that day.
  - Pre-processing of in-situ data: none

- Post-processing of gridded fields: none

- TXa is defined as TX but it is obtained without checking for consistency with the other variables.
  - Pre-processing of in-situ data: none
  - Post-processing of gridded fields: none

- TNa is defined as TN but it is obtained without checking for consistency with the other variables.
  - Pre-processing of in-situ data: none
  - Post-processing of gridded fields: none

- TXb is defined as TX and it is consistent with TM.
  - Pre-processing of in-situ data: none
  - Post-processing of gridded fields: TXb is consistent with TM and TNb, such that TNb $\leq$ TM $\leq$ TXb

- TNb is defined as TN and it is consistent with TM.
  - Pre-processing of in-situ data: none
  - Post-processing of gridded fields: TNb is consistent with TM and TXb, such that TNb $\leq$ TM $\leq$ TXb

A graphical representation of the variable definitions is shown in Fig. 1. For historical reasons, related to the way the observations were measured in the past, there are three different *day* definitions. Daily precipitation is aggregated over a period of 24 hours from 06 UTC of a day to 06 UTC of the day before, as a consequence hydrological applications require other quantities to be available with the same definition of day. Users interested in precipitation data may consider using the consistent set of variables RR, TG, TX and TN. Note that TX and TN are constrained by TG, despite the mismatch between the day definition of TG and that of the original daily extreme temperatures (see TXa and TNa in Fig. 1). For users interested in temperatures only, a better choice is the consistent set of variables TM, TXb and TNb. An additional advantage of using this set of variables is that the Norwegian data are aggregated over time in a way that is more consistent with the aggregations of Swedish and Finnish data. Finally, for users interested in daily minimum and maximum temperatures only, TXa and TNa are the two datasets obtained without any pre- or post- processing of the observed data. It is worth remarking that the spatial analyses of TXa and TNa are performed independently from each other, which means that there might be grid points, especially where the network is sparse, where TXa is smaller than TNa.

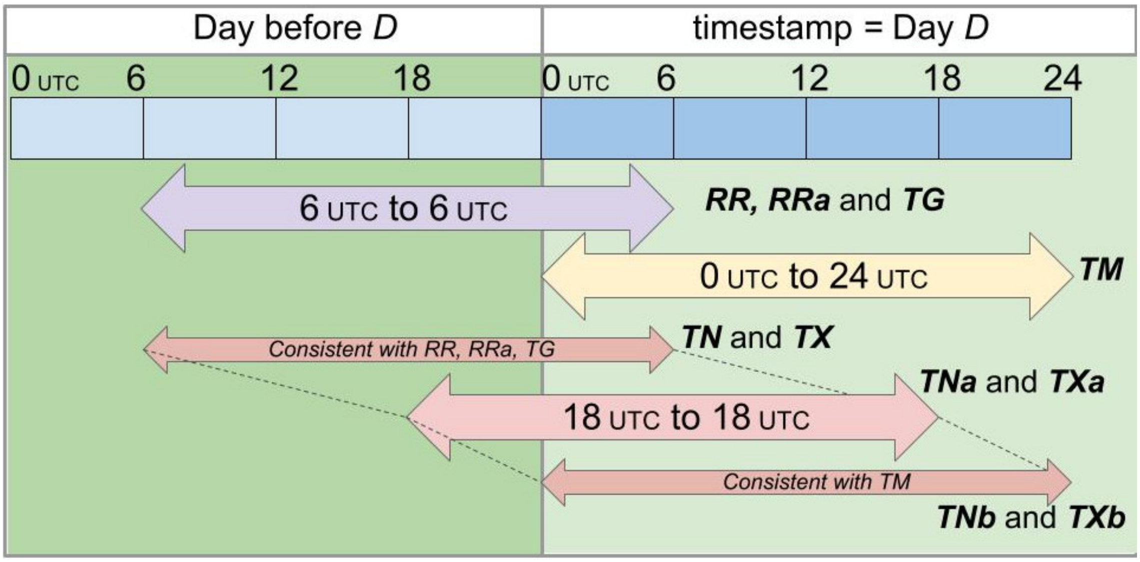

Figure 1: Definitions of daily variables.

The 64-year time period covered by the historical archive of v21 ranges from January 1957 to December 2020. The data availability is shown in Fig. 2 and it is compared against v20. The comparison of the spatial distribution of observations is shown in Figs. 3- 4. For all variables, there are significant variations in time of the number of observations as the observational network is constantly changing. In general, v21 uses more data than v20 in the early years of the period, from 1957 to 1975. Then, for RR, TN and TX the number of observations used is similar between the two versions. For the last two-three years, v21 uses more observations than v20, as can be seen also in Fig. 3, those are probably observations from the same observational networks that were not yet made available when preparing v20. In the case of TG and TM, from 2013 onward the time series of available observations for the two versions are very different and for v21 more observations are available, since we have aggregated to daily values a number of station data that were available as hourly values only. Fig. 4 shows that the additional observations are concentrated in South Norway and along the coast.

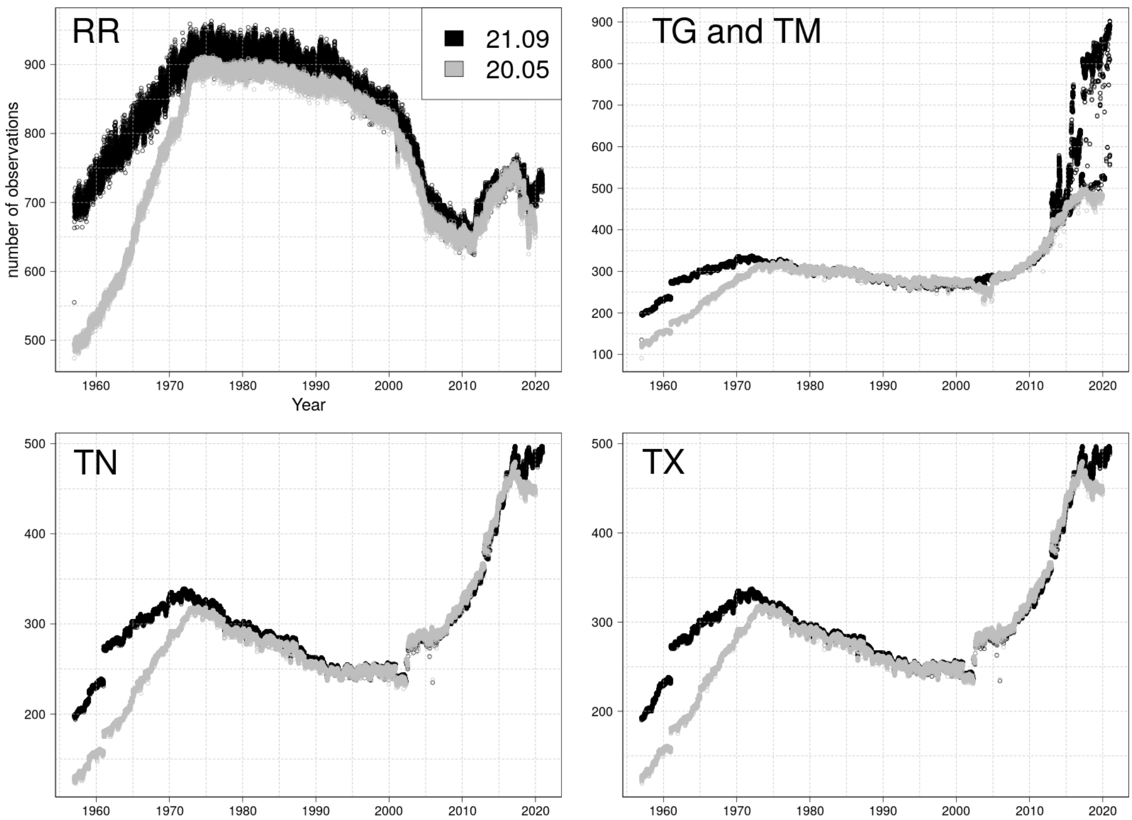

Figure 2: Time series of number of observations used for spatial analysis that are in the seNorge_2018 domain after the data quality control. The variable is indicated in the top right corner of each graph. The black dots refer to v21, while the gray dots are for v20. Note the different scales on the y-axes.

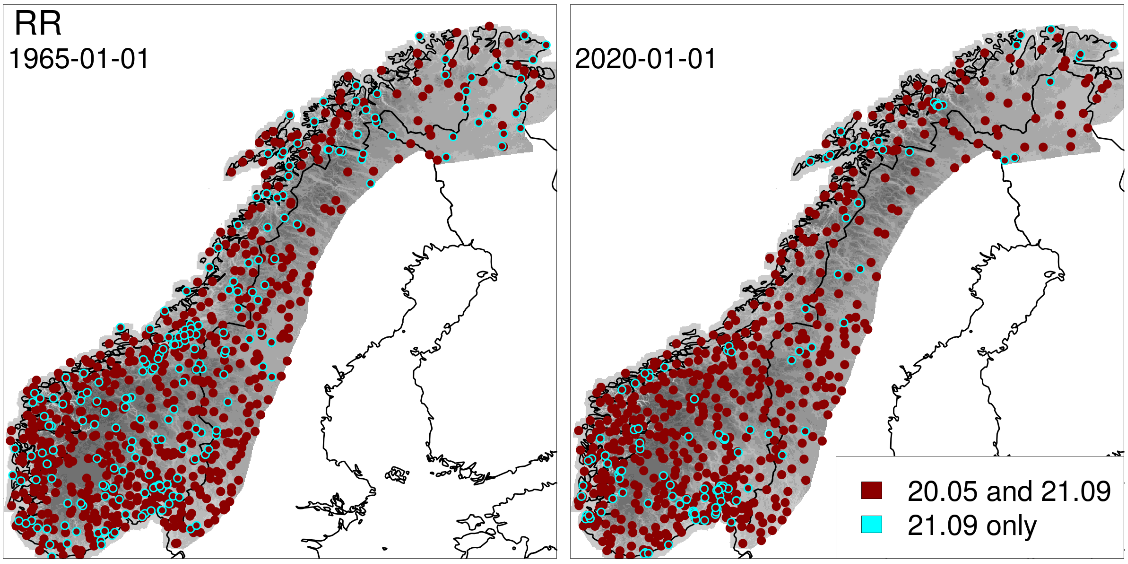

Figure 3: RR, Spatial distribution of the observational networks used for the two days reported in the panels. The observations used in v21 only are shown as cyan circles, the others are available for both versions.

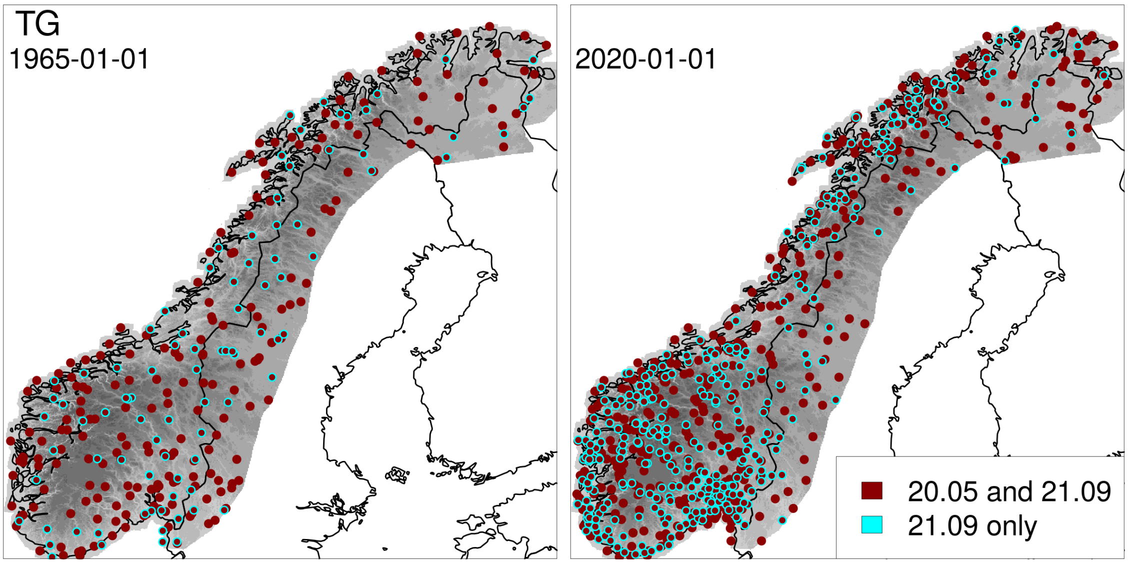

Figure 4: TG, Spatial distribution of the observational networks used for the two days reported in the panels. The observations used in v21 only are shown as cyan circles, the others are available for both versions.

3 Results

3.1 Comparison of v21 against v20

A comparison between v21 and v20 based on the 30-year period 1988-2017 is reported in this section for the four variables RR, TG, TX and TN. Our comparison aims at highlighting the systematic differences between the two versions and their main spatial patterns.

The strategy used is first to aggregate the daily values into monthly values. Then, for each month and grid point, the 30 monthly values are averaged into a single value representative of the typical value simulated at that point by the version used in the elaboration, the procedure is similar to the calculation of climate normals. For this reason, we refer to those typical fields as the climatologies of a version. The differences between v21 and v20 are assessed by studying the deviations between the climatologies. As stated above, our main interest is not to detect the local effects associated with individual observations that can enter the analysis or disappear from it. Instead, the assessment is on the impacts of variations of the observational network over a region that includes more than a few stations. For this reason, we have chosen to average the results of our comparison over boxes with sides of length 50 km. Note that for some parts of the domain, these boxes may still include only a few stations or even none. Figures 3 and 4 show that the highlands and forestry region in northern Sweden are not particularly well covered by the observational network we use.

The comparison of RR climatologies is shown in Fig. 5 for winter months and in Figs. 17- 19 for the other seasons. The results show the deviations between climatologies as percentages of v21 monthly values with respect to v20 values. For example, where the monthly total precipitation of v21 is approximately equal to the amount of v20 ($\pm$5%), then the corresponding square box is white. Green/blue (yellow/brown) colors indicate boxes where v21 have larger (smaller) precipitation amounts than v20. For the majority of the boxes the two versions are rather similar, that is $\pm$5% or $\pm$10%. However, for a few boxes (about 4) in the region of the Scandinavian mountains in northern Sweden, v21 is systematically drier than v20. In this region v21 has approximately 60%-70% of the amounts reported by v20. This could be the effect of some observations that are used in v21 only. In a region with a sparse observational network, even a few isolated stations can make a difference.

The comparison of TG climatologies is shown in Fig. 6 for winter months and in

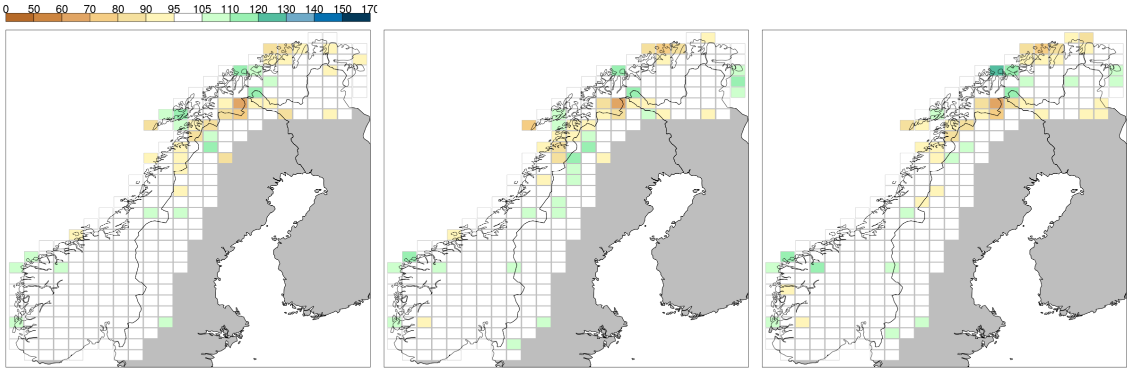

Figure 5: Monthly total precipitation climatologies of the winter months for seNorge_2018 v21, the values are shown as percentage of v20. Climatologies are computed over the 30-year period 1988-2017. The months: December, in the left panel; January, in the middle; February, in the right panel. The original 1 km fields of deviations are averaged over square boxes with sides of length 50 km.

Figs. 20- 22 for the other seasons. The only noteworthy differences occur during winter, while for the other season the box averages are almost everywhere ± 0.1°C. Fig. 6 shows that during winter v21 is a bit different from v20 on a number of boxes in the northern part of the domain (between ± 0.5°C and ± 1°C). The comparison of Fig. 6 with Fig. 5 shows that the difference patterns are quite similar to each other.

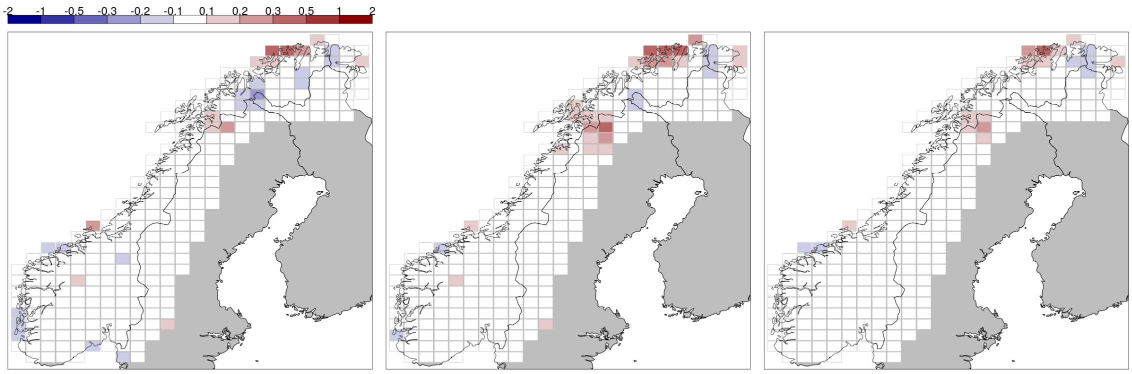

Figure 6: Differences between monthly mean TG climatologies of seNorge_2018 v21 and v20, units are °C. Climatologies are computed over the 30-year period 1988-2017. The months: December, in the left panel; January, in the middle; February, in the right panel. The original 1 km fields of deviations are averaged over square boxes with sides of length 50 km.

The comparison of TX climatologies is shown in Fig. 7 for winter months and Figs. 23-

25 for the other seasons. The two versions are similar, with very small deviations.

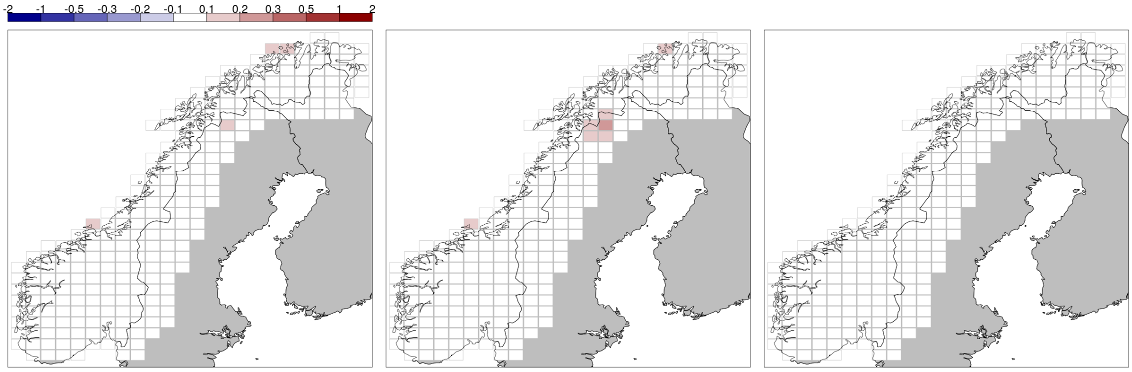

Figure 7: Differences between monthly mean TX climatologies of seNorge_2018 v21 and v20, units are °C. Climatologies are computed over the 30-year period 1988-2017. The months: December, in the left panel; January, in the middle; February, in the right panel. The original 1 km fields of deviations are averaged over square boxes with sides of length 50 km.

The comparison of TN climatologies is shown in Fig. 8 for winter months and Figs. 26-28 for the other seasons. The patterns and values of the deviations are similar to those of TG.

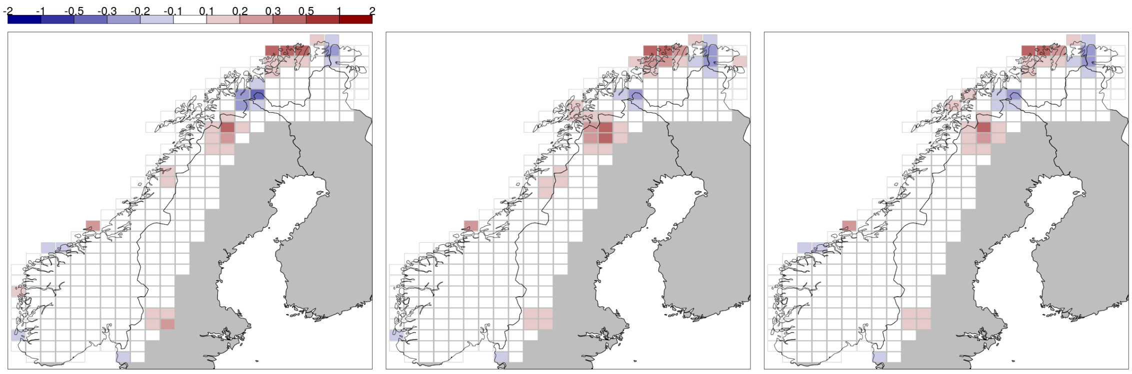

Figure 8: Differences between monthly mean TN climatologies of seNorge_2018 v21 and v20, units are °C. Climatologies are computed over the 30-year period 1988-2017. The months: December, in the left panel; January, in the middle; February, in the right panel. The original 1 km fields of deviations are averaged over square boxes with sides of length 50 km.

3.2 Comparison between v21 variables

The comparison between v21 variables described in this section is based on the 30-year period 1991-2020. The strategy adopted is similar to the one described in Sec. 3.1.

The climatologies of TM and TG have been compared to quantify the systematic differences between these two variables, which both represent daily mean temperatures. The deviations between monthly climatologies are shown in Figs. 9- 10 for spring. Similar figures for the other seasons are shown in Figs. 29- 34. Fig. 9 shows the spatial patterns of the differences between TM and TG. Fig. 10 shows the same deviations as a function of the TG climatological value. Note that in Fig. 10, the original values on the 1 km grid have been used (i.e. there is no averaging over the 50 km square boxes).

The data analysis shows that the deviations between TG and TM vary in space and time and that the systematic differences are in the range of -0.5C to $+0.7$C. During winter, TM and TG have similar typical values, as shown in Figs. 29- 30. Even though in February, TM is warmer than TG in south-east Norway and inland in northern Norway. Spring is the season where TM and TG differ the most. TM is warmer than TG almost everywhere, as shown in Figs. 9- 10. The largest deviations between TM and TG lie in the range from $+0.4$C to $+0.7$C, although for most of the points they lie between $+0.2$C and $+0.4$C. It is interesting to note that during autumn (Figs. 33- 34) the situation is the opposite over the continental regions in Sweden and Finland, where TM is colder than TG, although the absolute values of the differences are smaller than during spring. Summer is shown in Figs. 31- 32 and in this season the patterns of the deviations between TM and TG gradually change between those seen in spring and those in autumn, as one may expect.

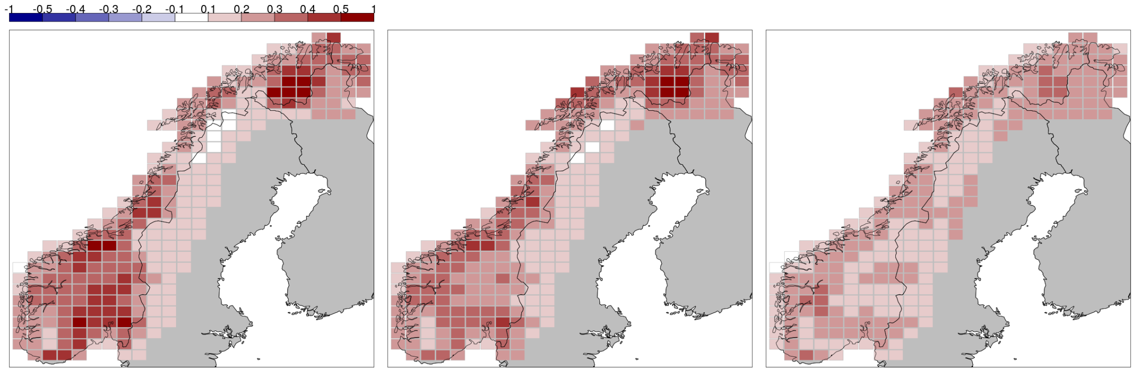

Figure 9: seNorge_2018 v21, differences between monthly normals of TM and TG (TM minus TG), as °C. Climatologies are computed over the 30-year period 1991-2020. The months shown are: March, in the left panel; April, in the middle; May, in the right panel. The original 1 km fields of deviations are averaged over square boxes with sides of length 50 km.

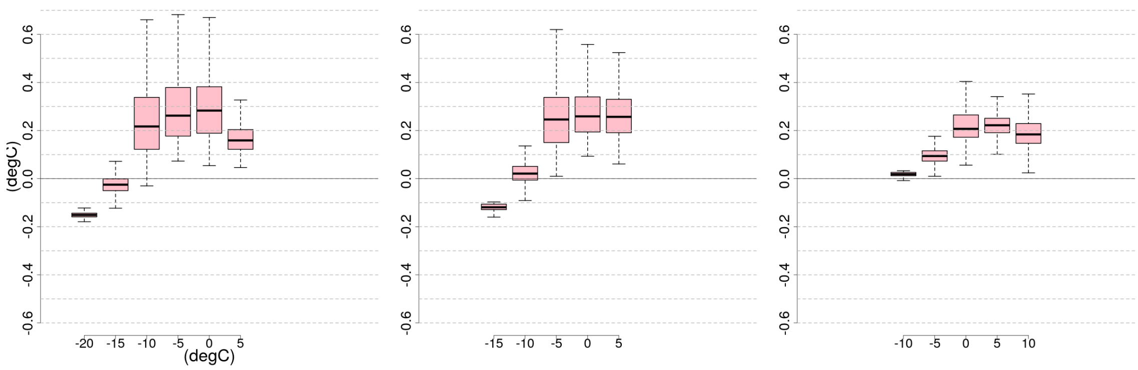

Figure 10: seNorge_2018 v21, differences between monthly normals of TM and TG (TM-TG) as a function of TG monthly normals. Units are °C. Climatologies are computed over the 30-year period 1991-2020. The months shown are: March, in the left panel; April, in the middle; May, in the right panel. The boxplots are based on the original fields over the 1 km grid.

The comparison of RR and RRa is described in this paragraph. RRa is the precipitation as it has been observed by the rain gauges. RR is the precipitation adjusted for the wind-induced undercatch, which also depends on the daily mean temperature. Then, wind speed and temperature are required at each gridpoint. For seNorge_2018, we have used the wind speed derived from numerical model output and the TG fields. At observation locations, RR is always equal or greater than RRa. At grid points, RR should be equal or greater than RRa, although occasionally it can happen that RR is smaller than RRa because of interpolation artifacts. The deviations between RR and RRa climatologies are shown for winter months in Figs. 11- 12. The relative difference between RR and RRa is shown in the figures. Similar figures for the other seasons are shown in Figs. 35- 40.

The relationship between temperature and RR adjustments is rather evident both in the seasonality and in the spatial distribution of the adjustments. During summer, RR is equal to RRa or just slightly larger, up to 10% bigger. In winter, the adjustments are quite significant everywhere, especially in some regions of northern Norway where RR can be 60% larger than RRa. Note that Fig. 11 shows that along the coast the adjustments tend to be around 10% and 20% even during winter, except for the northernmost part of Norway.

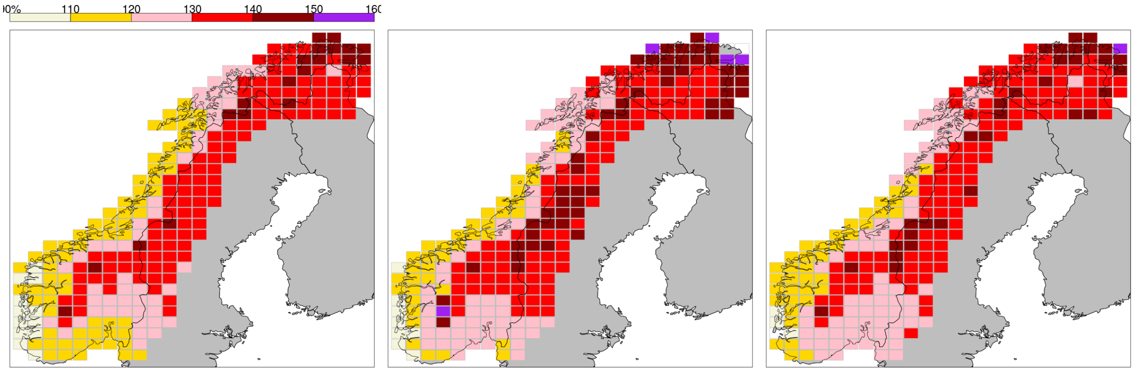

Figure 11: seNorge_2018 v21, differences between monthly totals of RR and RRa expressed as percentage of RRa (100 · RR/RRa). Units are %. The 30-year time period considered ranges from 1991 to 2020. The months shown are: December, in the left panel; January, in the middle; February, in the right panel. The original 1 km fields of deviations are averaged over square boxes with sides of length 50 km.

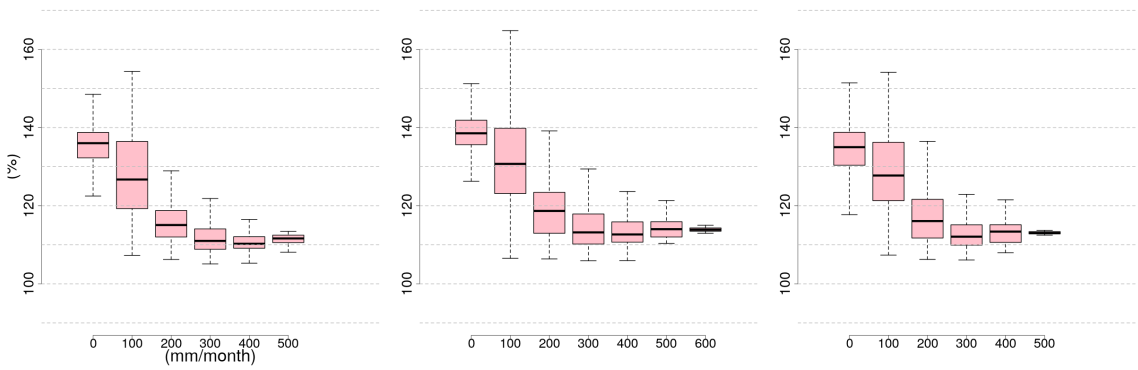

Figure 12: seNorge_2018 v21, differences between monthly totals of RR and RRa (100 · RR/RRa) as a function of RRa on the x-axis. X-axis units are *mm*. Y-axis units are %. The 30-year time period considered ranges from 1991 to 2020. The months shown are: December, in the left panel; January, in the middle; February, in the right panel. The boxplots are based on the original fields over the 1 km grid.

The comparison between the different variables of daily minimum and maximum temperatures is described in this paragraph. TXa and TNa are the results of the spatial analysis of the observed temperatures and they are used as a reference to assess the effects of the post-processing.

The differences between TXb and TXa are not shown because they are between $\pm 0.1°C$ for all months. The same situation happens for the differences between TNb and TNa.

The differences between TX and TXa climatologies are shown in Figs. 13- 14 and the differences between TN and TNa climatologies are shown in Figs. 15- 16 for the winter months. For the other months, the same differences are between ±0.1°C. The effects of the post-processing do have systematic impacts on the deviations between daily extreme temperatures only over the regions between Norway and Sweden and Norway and Finland, where the stations coverage is sparser and the uncertainties associated with the interpolation are greater. In those regions, TX is approximately 1-2% higher than the predicted value for TXa and TN is 1-2% lower than TNa, as it can be seen in Figs. 14- 16.

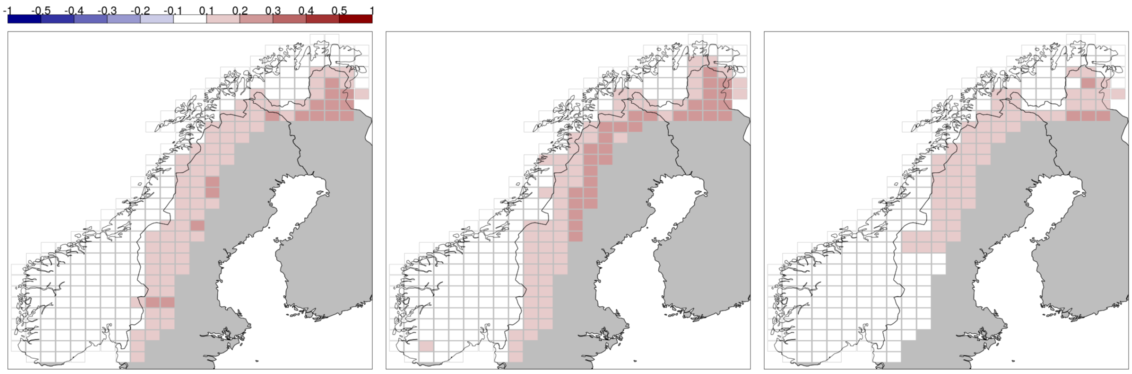

Figure 13: seNorge_2018 v21, differences between monthly normals of TX and TXa (TX minus TXa), as °C. Climatologies are computed over the 30-year period 1991-2020. The months shown are: December, in the left panel; January, in the middle; February, in the right panel. The original 1 km fields of deviations are averaged over square boxes with sides of length 50 km.

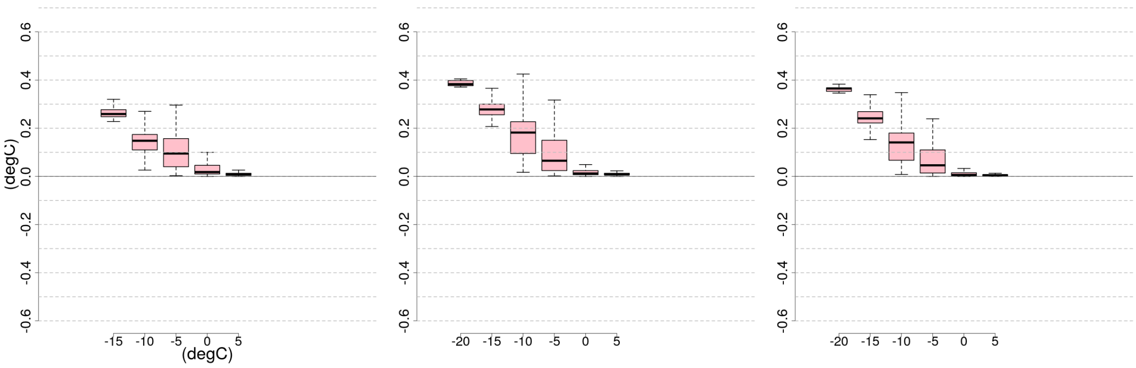

Figure 14: seNorge_2018 v21, differences between monthly normals of TX and TXa (TX minus TXa) as a function of TXa monthly normals. Units are °C. Climatologies are computed over the 30-year period 1991-2020. The months shown are: December, in the left panel; January, in the middle; February, in the right panel. The boxplots are based on the original fields over the 1 km grid.

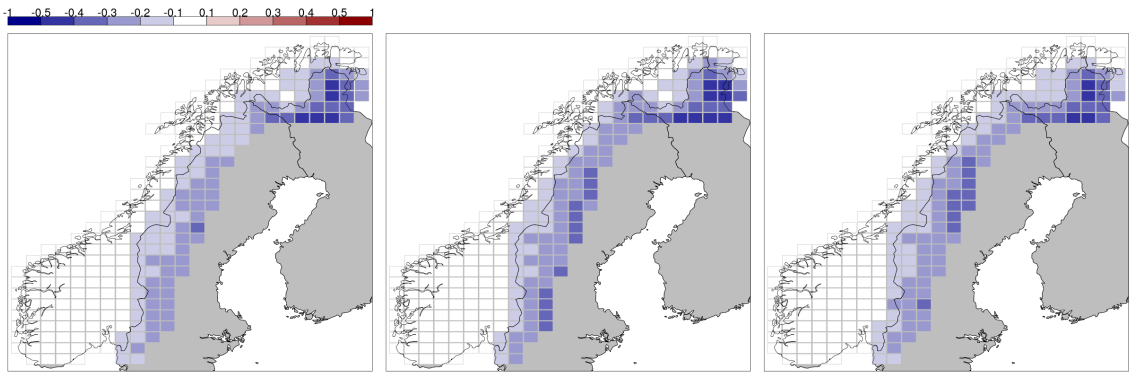

Figure 15: seNorge_2018 v21, differences between monthly normals of TN and TNa (TN minus TNa), as °C. Climatologies are computed over the 30-year period 1991-2020. The months shown are: December, in the left panel; January, in the middle; February, in the right panel. The original 1 km fields of deviations are averaged over square boxes with sides of length 50 km.

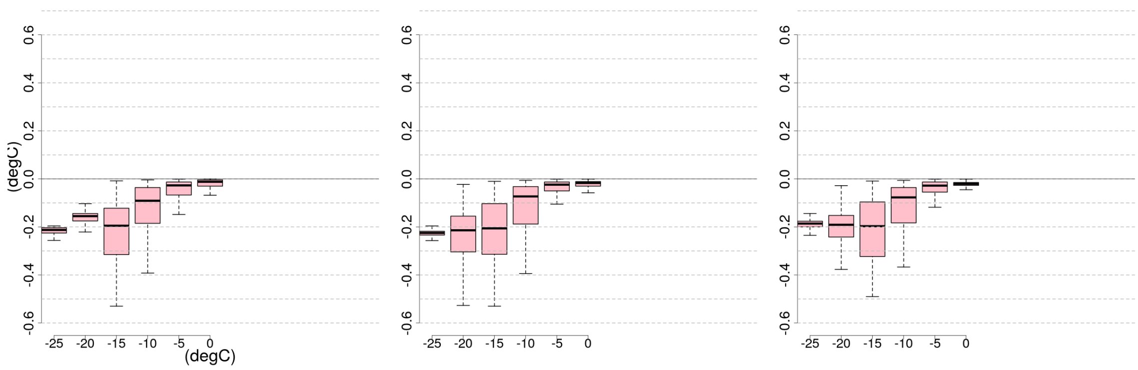

Figure 16: seNorge_2018 v21, differences between monthly normals of TN and TNa (TN minus TNa) as a function of TNa monthly normals. Units are °C. Climatologies are computed over the 30-year period 1991-2020. The months shown are: December, in the left panel; January, in the middle; February, in the right panel. The boxplot are based on the original fields over the 1 km grid.

4 Conclusions

seNorge_2018 v21 is an update on v20 covering the most recent time period. With respect to v20, v21 contains more variables. The new variables allow a more consistent description for daily temperature and precipitation on the aggregation interval chosen by the users.

The data sources for the in-situ observations are the same for the two versions. v21 uses more observations than v20, especially from 1957 to 1975. For the daily mean temperatures, from 2013 up to the period included in the operational archive, the number of observations used in v21 is significantly higher than for v20. The additional observations are mostly located in South Norway and along the Norwegian coast. On the one hand, the increase in observation density allows for a better description of small-scale processes. On the other hand, an observational network that is changing significantly in time makes the comparison of the gridded fields for different periods more complex to interpret.

The comparison of the gridded fields of v21 and v20 on a common time period shows that the new version is very much consistent with the previous one. There are some differences for a small region on the border between Sweden and Norway and for the northernmost part of the domain, both regions are not well covered by in-situ observations.

We have compared v21 variables that aim to represent similar quantities with the objective to quantify their differences.

TM is often warmer than TG over the Norwegian mainland.

The deviations between RR and RRa quantify the impact of the adjustment for the wind-induced under-catch. During the warmest months, that is from May to September, the adjustment is limited and RR is greater than RRa by about 10% at most. In the coldest months, the adjustment is more consistent, especially in the regions experiencing the coldest temperatures where RR exceeds RRa by 40% or 50% of its value. Note that the most significant adjustments occur where the typical precipitation values are among the lowest registered on the domain, while where precipitation is greater, the adjustment is still around 10%.

The variables representing the daily minimum and maximum temperatures are quite similar to each other. The only systematic differences between TX/TN and the other variables are related to border effects of the interpolation where the observational network is sparse.

Appendix: Data Access

seNorge_2018 v21 datasets are available for public download under the Norwegian Licence for Open Government Data (NLOD, https://data.norge.no/nlod/en/). The data can be accessed from two distinct sources: Zenodo zenodo.org and MET's Norway THREDDS data server thredds.met.no. A detailed description on how to access the data is available at the seNorge wiki-pages:

- https://github.com/metno/seNorge_docs/wiki/seNorge_2018

The wiki is a live documentation where it is also possible to get the latest news and contact the developers by opening issues about specific topics.

The datasets used in this document are:

- TG. https://doi.org/10.5281/zenodo.5205509
- TM. https://doi.org/10.5281/zenodo.5216013
- TX. https://doi.org/10.5281/zenodo.5552961
- TXa. https://doi.org/10.5281/zenodo.5552970
- TXb. https://doi.org/10.5281/zenodo.5552971
- TN. https://doi.org/10.5281/zenodo.5552974
- TNa. https://doi.org/10.5281/zenodo.5552975
- TNb. https://doi.org/10.5281/zenodo.5552978
- RR. https://doi.org/10.5281/zenodo.5205515
- RRa. https://doi.org/10.5281/zenodo.5205515

Supplementary Material

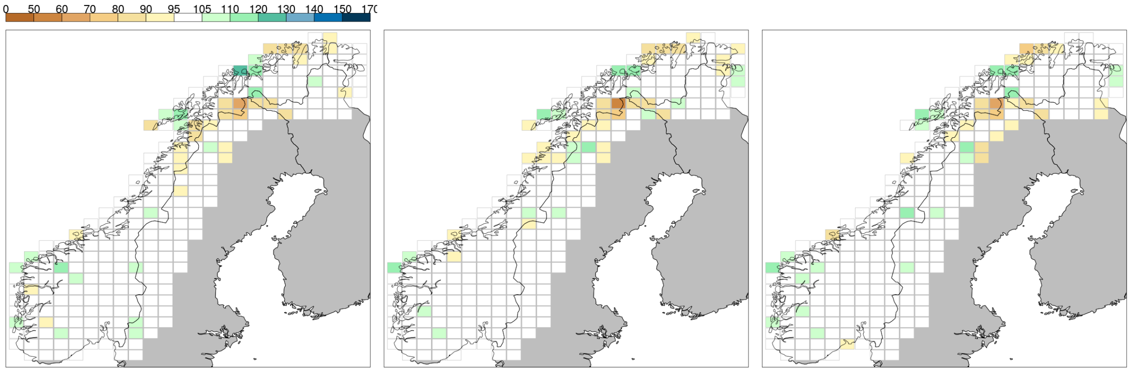

Figure 17: Same as Fig. 5 but for spring months: March, in the left panel; April, in the middle; May, in the right panel.

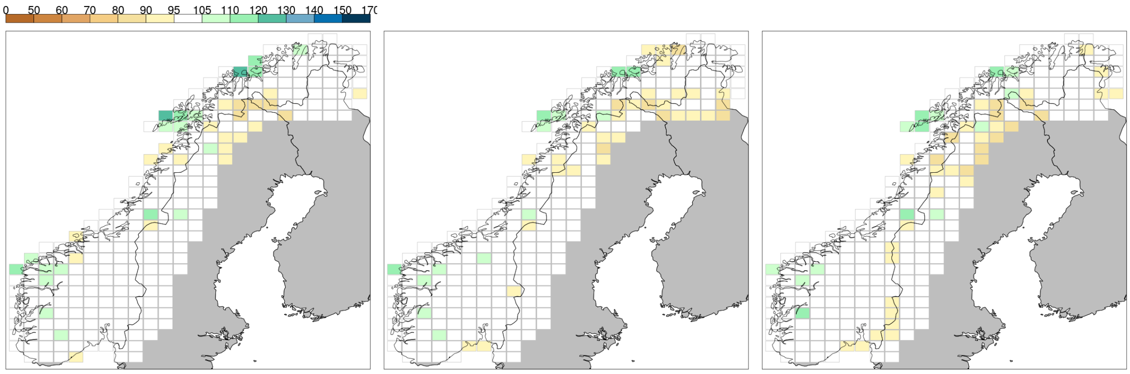

Figure 18: Same as Fig. 5 but for summer months: June, in the left panel; July, in the middle; August, in the right panel.

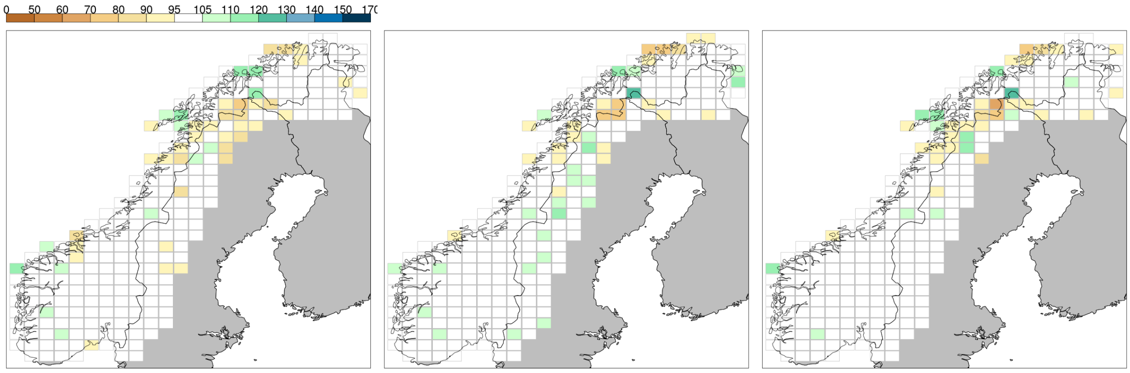

Figure 19: Same as Fig. 5 but for autumn months: September, in the left panel; October, in the middle; November, in the right panel.

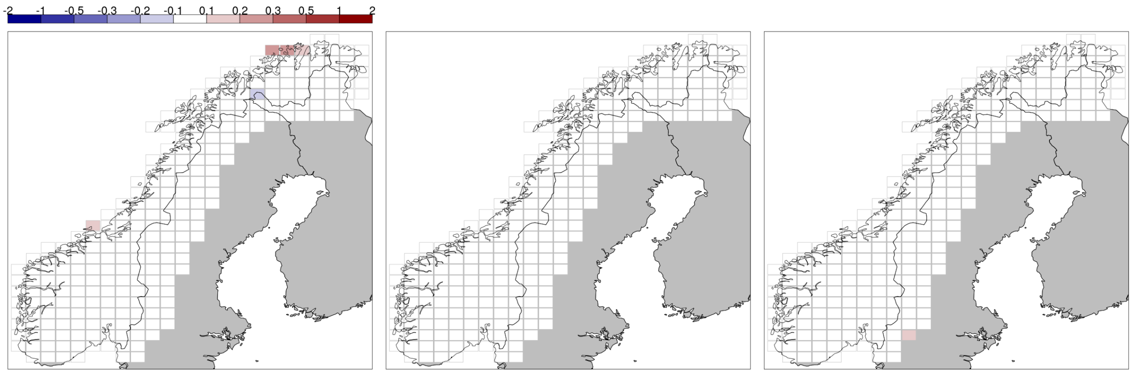

Figure 20: Same as Fig. 6 but for spring months: March, in the left panel; April, in the middle; May, in the right panel.

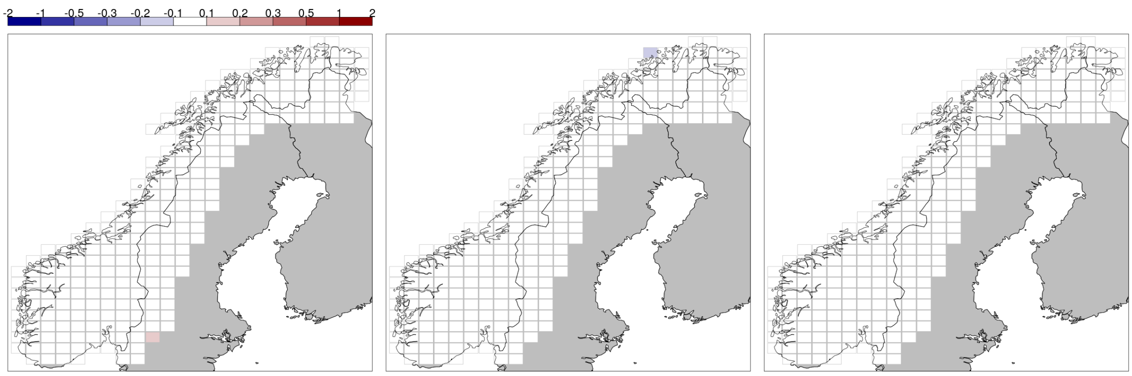

Figure 21: Same as Fig. 6 but for summer months: June, in the left panel; July, in the middle; August, in the right panel.

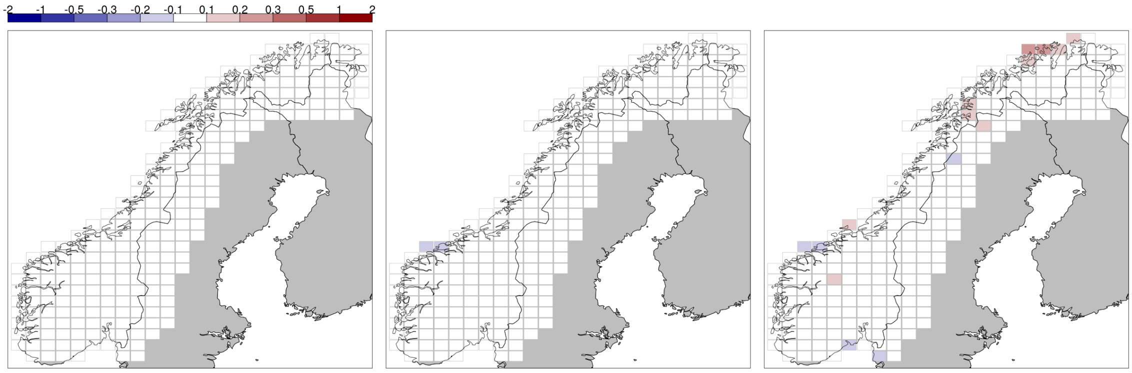

Figure 22: Same as Fig. 6 but for autumn months: September, in the left panel; October, in the middle; November, in the right panel.

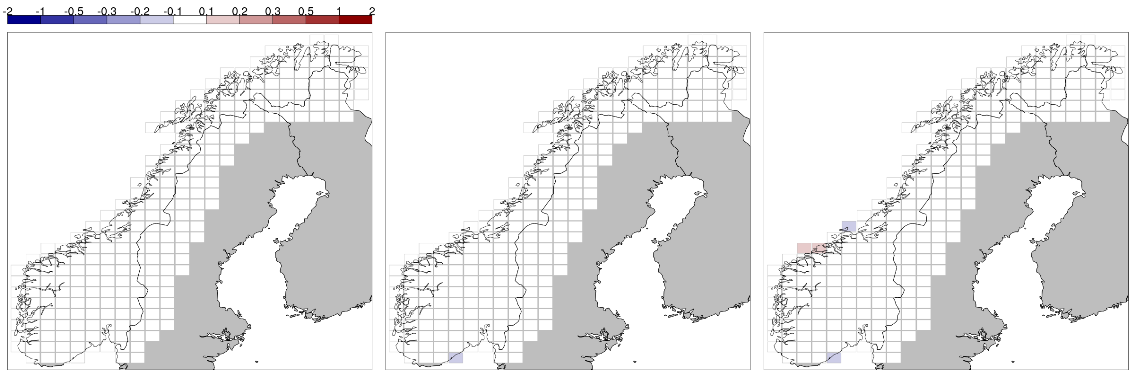

Figure 23: Same as Fig. 7 but for spring months: March, in the left panel; April, in the middle; May, in the right panel.

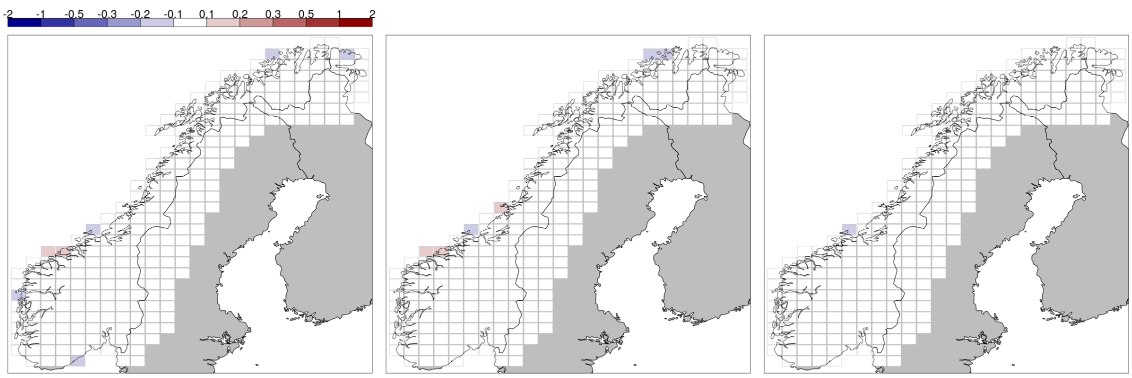

Figure 24: Same as Fig. 7 but for summer months: June, in the left panel; July, in the middle; August, in the right panel.

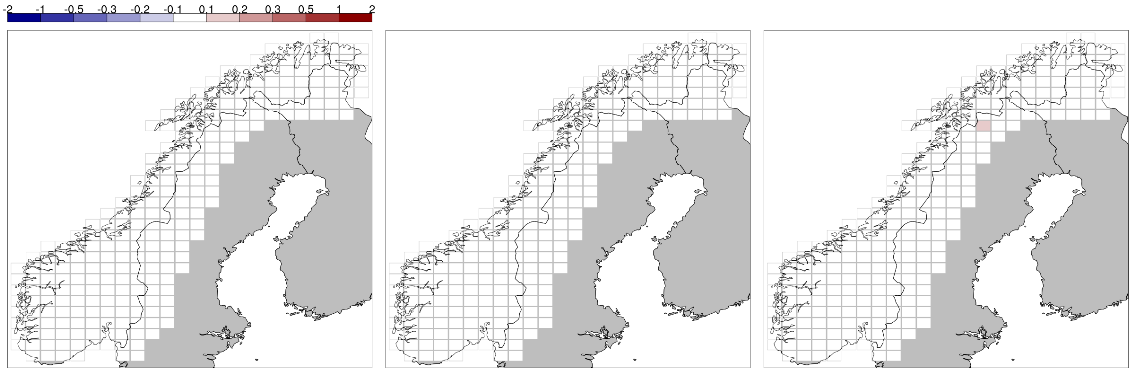

Figure 25: Same as Fig. 7 but for autumn months: September, in the left panel; October, in the middle; November, in the right panel.

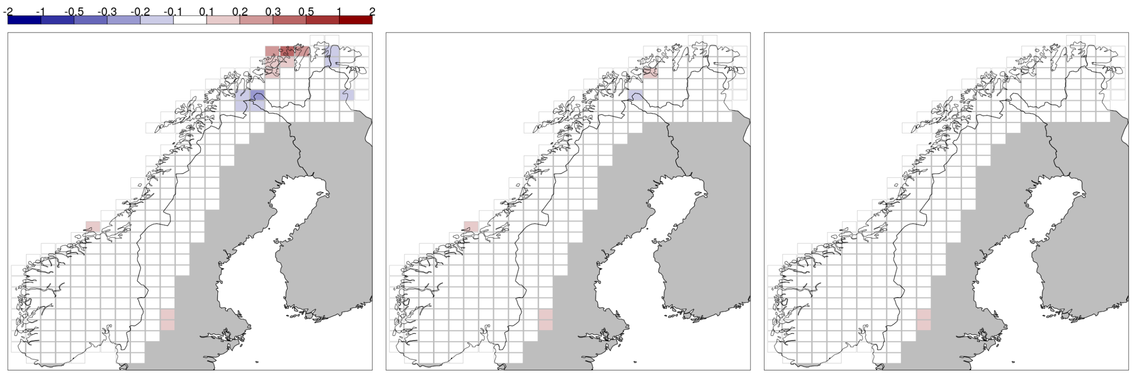

Figure 26: Same as Fig. 8 but for spring months: March, in the left panel; April, in the middle; May, in the right panel.

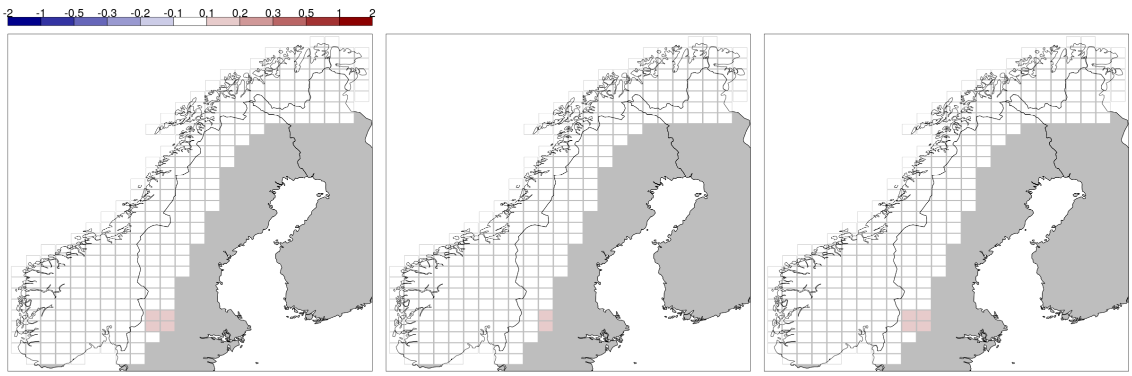

Figure 27: Same as Fig. 8 but for summer months: June, in the left panel; July, in the middle; August, in the right panel.

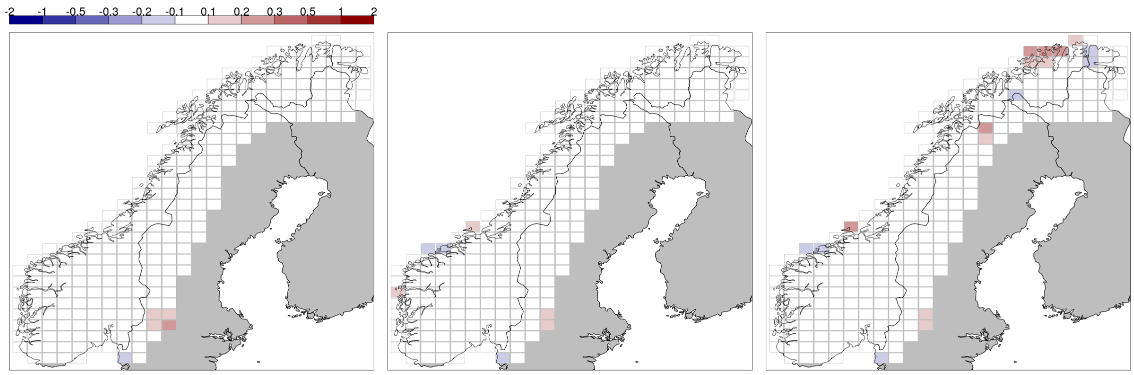

Figure 28: Same as Fig. 8 but for autumn months: September, in the left panel; October, in the middle; November, in the right panel.

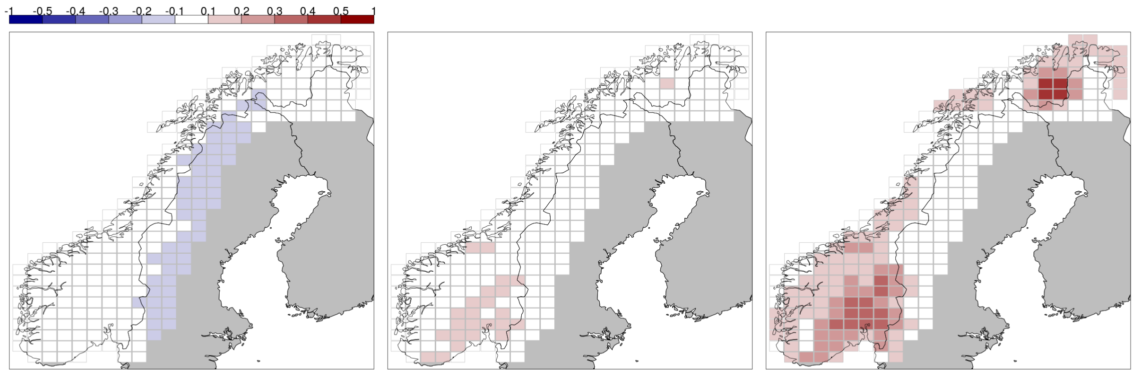

Figure 29: Same as Fig. 9 but for winter months: December, in the left panel; January, in the middle; February, in the right panel.

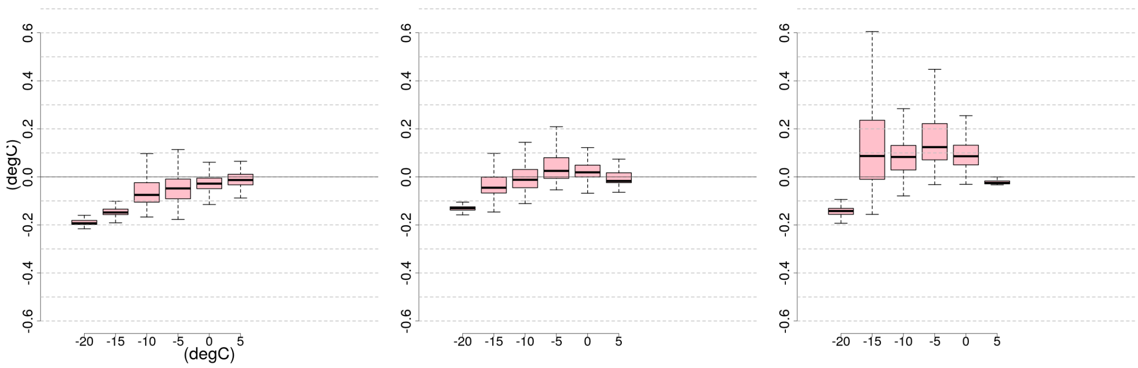

Figure 30: Same as Fig. 10 but for winter months: December, in the left panel; January, in the middle; February, in the right panel.

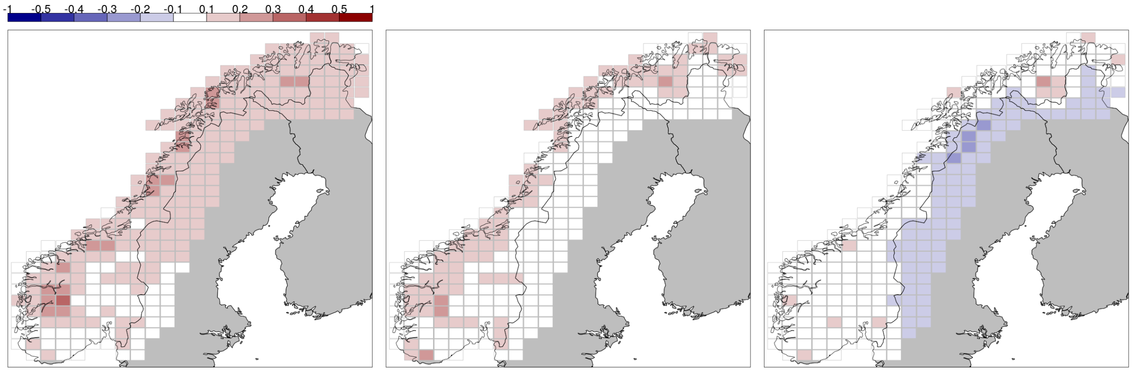

Figure 31: Same as Fig. 9 but for summer months: June, in the left panel; July, in the middle; August, in the right panel.

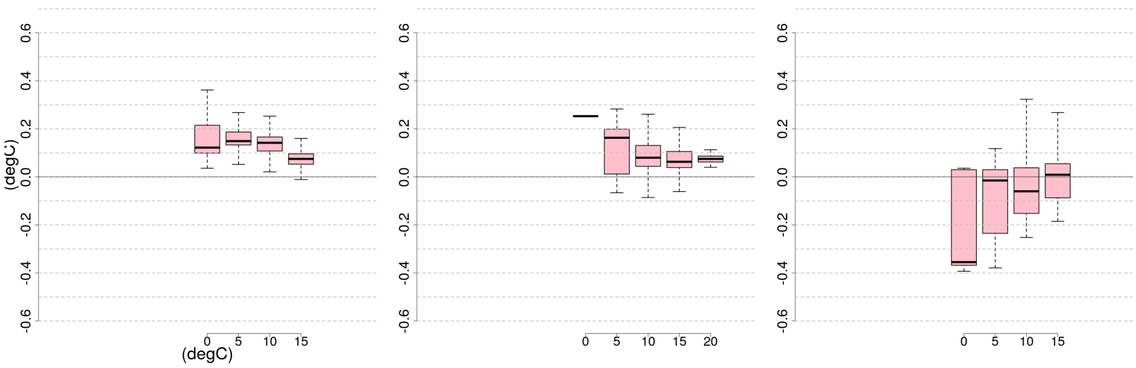

Figure 32: Same as Fig. 10 but for summer months: June, in the left panel; July, in the middle; August, in the right panel.

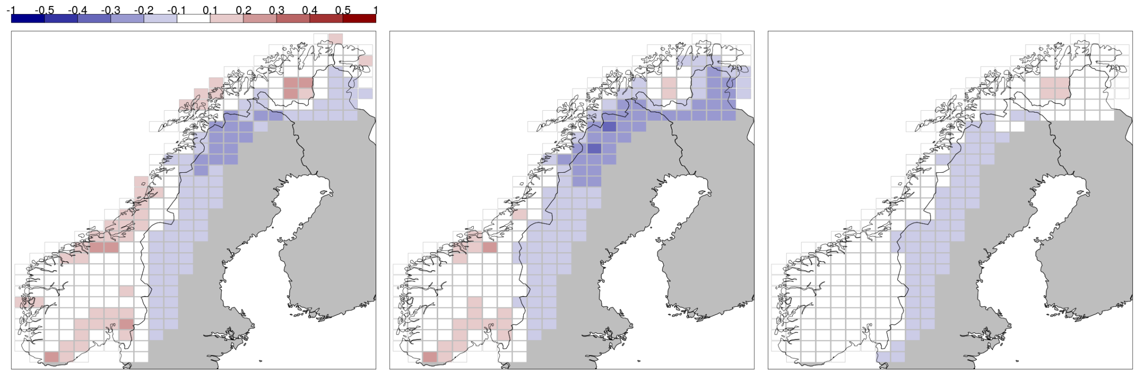

Figure 33: Same as Fig. 9 but for autumn months: September, in the left panel; October, in the middle; November, in the right panel.

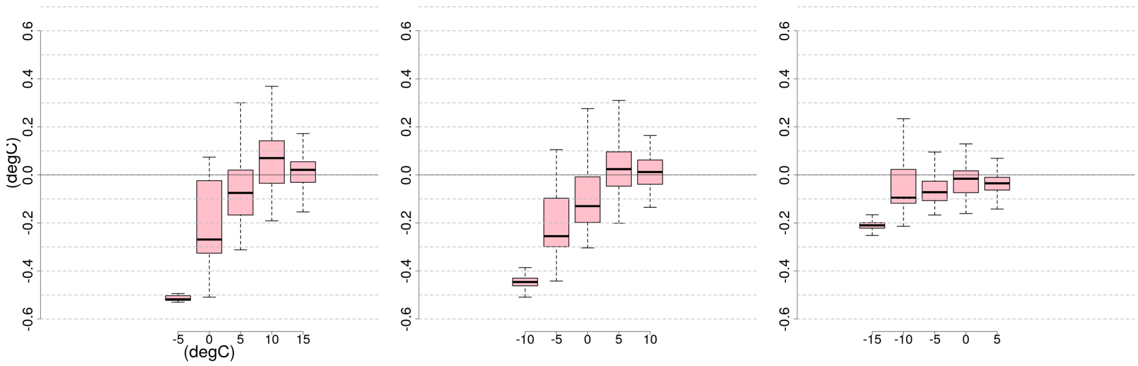

Figure 34: Same as Fig. 10 but for autumn months: September, in the left panel; October, in the middle; November, in the right panel.

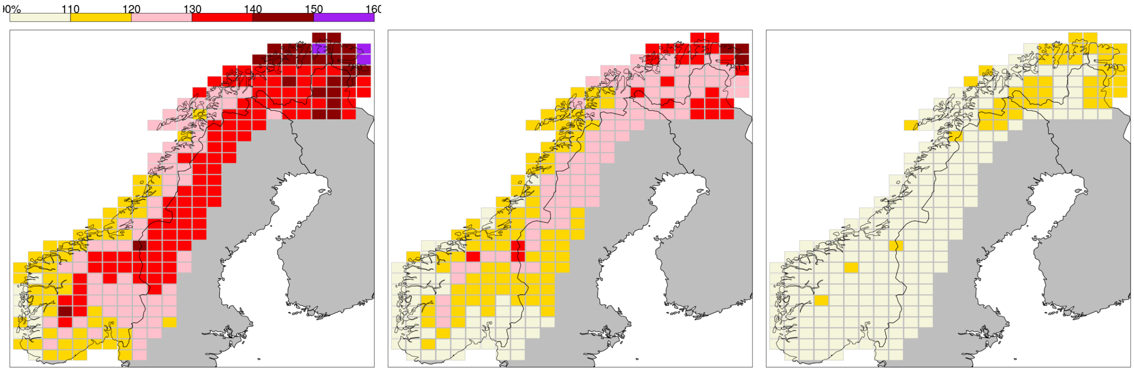

Figure 35: Same as Fig. 11 but for spring months: March, in the left panel; April, in the middle; May, in the right panel.

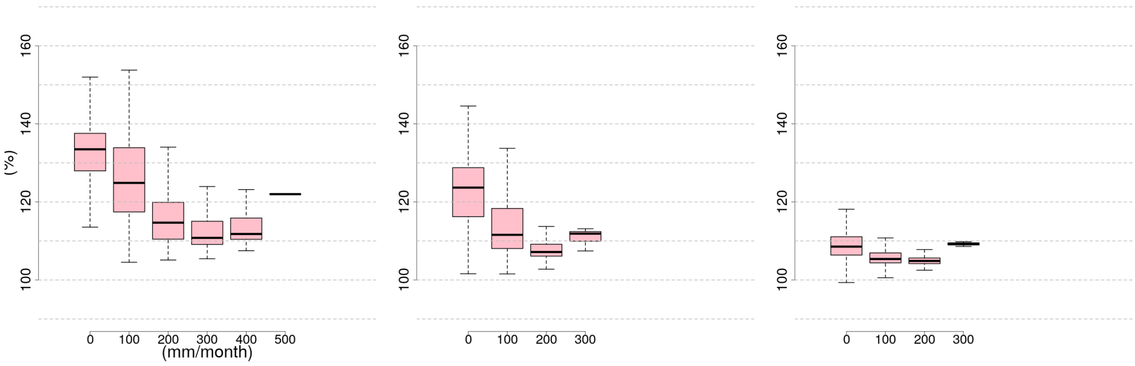

Figure 36: Same as Fig. 12 but for spring months: March, in the left panel; April, in the middle; May, in the right panel.

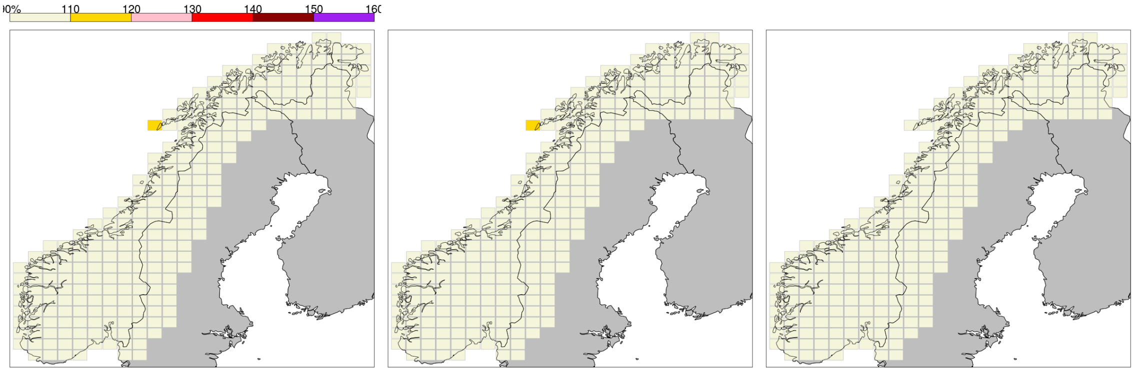

Figure 37: Same as Fig. 11 but for summer months: June, in the left panel; July, in the middle; August, in the right panel.

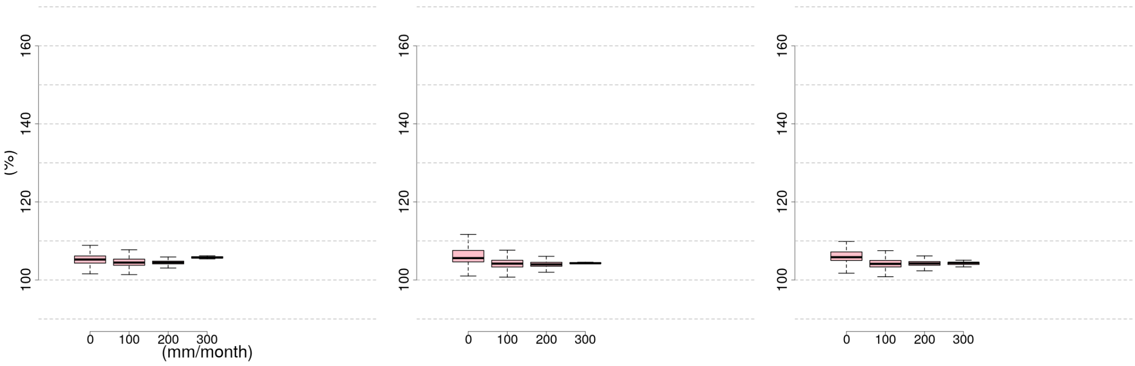

Figure 38: Same as Fig. 12 but for summer months: June, in the left panel; July, in the middle; August, in the right panel.

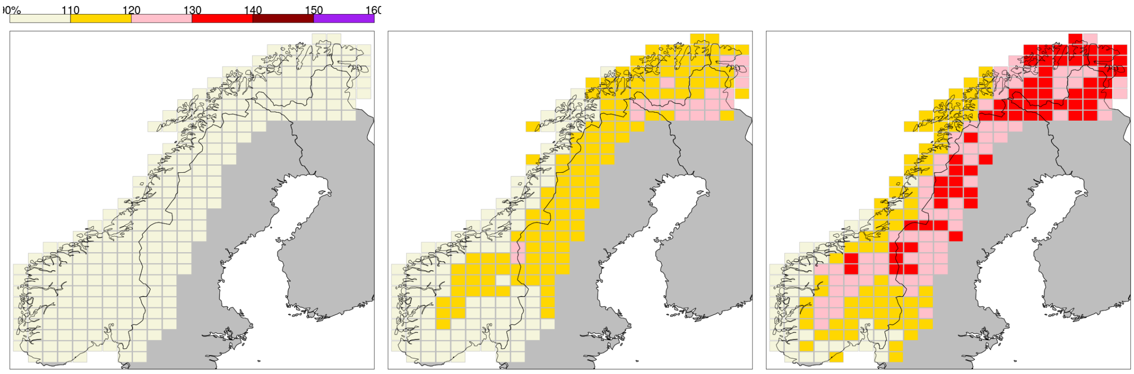

Figure 39: Same as Fig. 11 but for autumn months: September, in the left panel; October, in the middle; November, in the right panel.

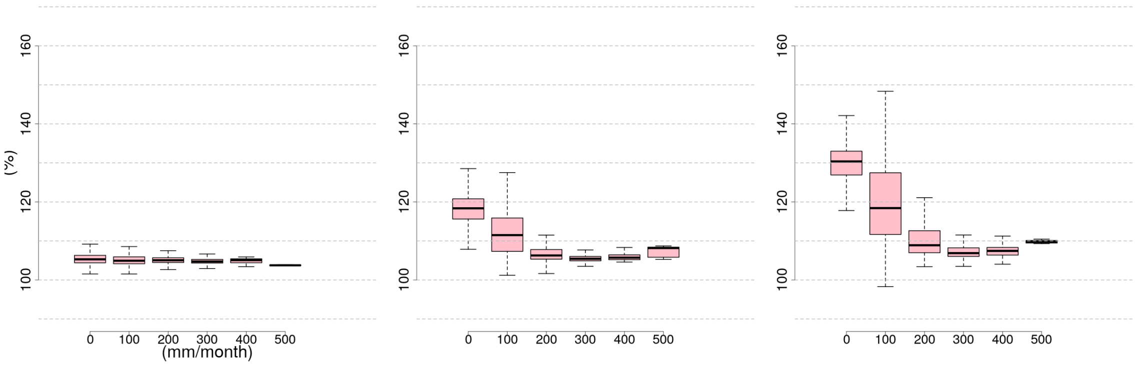

Figure 40: Same as Fig. 12 but for autumn months: September, in the left panel; October, in the middle; November, in the right panel.

References

Båserud, L., C. Lussana, T. N. Nipen, I. A. Seierstad, L. Oram, and T. Aspelien (2020), Titan automatic spatial quality control of meteorological in-situ observations, *Advances in Science and Research*, *17*, 153–163, doi:10.5194/asr-17-153-2020.

Førland, E., and O. Tveito (1997), Temperatur og snødata for flomberegning, *DNMI Report*, *28*(97), 51.

Klein Tank, A., J. Wijngaard, G. Können, R. Böhm, G. Demarée, A. Gocheva, M. Mileta, S. Pashiardis, L. Hejkrlik, C. Kern-Hansen, et al. (2002), Daily dataset of 20th-century surface air temperature and precipitation series for the European climate assessment, *International journal of climatology*, *22*(12), 1441–1453.

Lussana, C. (2020), senorge observational gridded datasets. senorge_2018, version 20.05.

Lussana, C., F. Uboldi, and M. R. Salvati (2010), A spatial consistency test for surface observations from mesoscale meteorological networks, *Quarterly Journal of the Royal Meteorological Society*, *136*(649), 1075–1088.

Lussana, C., T. Saloranta, T. Skaugen, J. Magnusson, O. E. Tveito, and J. Andersen (2018a), seNorge2 daily precipitation, an observational gridded dataset over Norway from 1957 to the present day, *Earth System Science Data*, *10*(1), 235–249, doi: 10.5194/essd-10-235-2018.

Lussana, C., O. E. Tveito, and F. Uboldi (2018b), Three-dimensional spatial interpolation of 2m temperature over Norway, *Quarterly Journal of the Royal Meteorological Society*, *144*(711), 344–364, doi:10.1002/qj.3208.

Lussana, C., O. E. Tveito, A. Dobler, and K. Tunheim (2019), senorge_2018, daily precipitation, and temperature datasets over norway, *Earth System Science Data*, *11*(4), 1531–1551, doi:10.5194/essd-11-1531-2019.

Mohr, M. (2008), New routines for gridding of temperature and precipitation observations for "senorge. no", *Met. no Report*, *8*, 2008.

Tveito, O., E. Førland, R. Heino, I. Hanssen-Bauer, H. Alexandersson, B. Dahlström, A. Drebs, C. Kern-Hansen, T. Jónsson, E. Vaarby Laursen, et al. (2000), Nordic temperature maps, *DNMI report*, *9*(00).

Tveito, O. E., and E. J. Førland (1999), Mapping temperatures in Norway applying terrain information, geostatistics and GIS, *Norsk Geografisk Tidsskrift-Norwegian Journal of Geography*, *53*(4), 202–212.

Tveito, O. E., H.-C. Udnæs, Z. Mengistu, R. Engeset, and E. J. Førland (2002), New snow maps for Norway, in *Proceedings XXII Nordic Hydrological Conference 2002*, pp. 527–532.

Tveito, O. E., I. Bjørdal, A. O. Skjelvåg, and B. Aune (2005), A gis-based agro-ecological decision system based on gridded climatology, *Meteorological Applications*, *12*(1), 57–68.

Wolff, M. A., K. Isaksen, A. Petersen-Øverleir, K. Ødemark, T. Reitan, and R. Brækkan (2015), Derivation of a new continuous adjustment function for correcting wind-induced loss of solid precipitation: results of a norwegian field study, *Hydrology and Earth System Sciences*, *19*(2), 951–967, doi:10.5194/hess-19-951-2015.